

Reconfiguration Dynamics in folded and intrinsically disordered protein with internal friction: Effect of solvent quality and denaturant

Nairhita Samanta and Rajarshi Chakrabarti*

Department of Chemistry, Indian Institute of Technology Bombay,

Mumbai, Powai 400076, E-mail: rajarshi@chem.iitb.ac.in

(Dated: April 5, 2024)

We consider a phantom chain model of polymer with internal friction in a harmonic confinement and extend it to take care of effects of solvent quality following a mean field approach where an exponent ν is introduced. The model termed as “Solvent Dependent Compacted Rouse with Internal Friction (SDCRIF)” is then used to calculate the reconfiguration time of a chain that relates to recent Förster resonance energy transfer (FRET) studies on folded and intrinsically disordered proteins (IDPs) and can account for the effects of solvent quality as well as the denaturant concentration on the reconfiguration dynamics. Following an ansatz that relates the strength of the harmonic confinement (k_c) with the internal friction of the chain (ξ_{int}), SDCRIF can convincingly reproduce the experimental data and explain how the denaturant can change the time scale for the internal friction. It can also predict near zero internal friction in case of IDPs. In addition, our calculations show that the looping time as well as the reconfiguration time scales with the chain length N as $\sim N^\alpha$, where α depends weakly on the internal friction but has rather stronger dependence on the solvent quality. In absence of any internal friction, $\alpha = 2\nu + 1$ and it goes down in presence of internal friction, but looping slows down in general. On the contrary, poorer the solvent, faster the chain reconfigures and forms loop, even though one expects high internal friction in the collapsed state. However, if the internal friction is too high then the looping and reconfiguration dynamics become slow even in poor solvent.

I. INTRODUCTION

Among the polymer rheologists the notion of internal friction associated with a single polymer chain is more than twenty five years old [1–4]. Surprisingly it is only very recently that the topic has gained attention in the chemical and biophysics community. Although some earlier works in chemical physics community did point out the importance of internal friction in single chain dynamics [5, 6] but did not receive the attention it should have. However recent experiments on looping and folding dynamics [7–12] in proteins have indicated the non-negligible role of internal friction. In this context it is worth mentioning that loop formation between any two parts of a bio-polymer [13–24] is supposedly the primary step of protein folding, DNA cyclization and since internal friction affects looping it is obvious that measurements of folding rates in proteins would predict the importance of solvent independent internal friction as well [25]. Subsequently not only these recent experiments [11, 12, 26] on polypeptides and proteins showed internal friction to play a pivotal role in the dynamics but also motivated theoretical chemical physicists to come up with statistical mechanical models for single polymer chain with the inclusion of internal friction [27–31] and apply these models to investigate the loop formation dynamics. Other than model build up there have been attempts to elucidate the origin of internal friction in proteins based on computer simulation studies [32–38]. A careful literature survey would reveal that it was de Gennes [39], who introduced the concept of internal viscosity at the single chain level. Rabin and Öttinger proposed an expression for the relaxation time, τ_{rel} associated with internal viscosity following an idea of de Gennes [39], which is $\tau_{rel} = R^3/k_B T(\eta_s + \eta_i)$ where, $R = aN^\nu$ and a , N are the monomer size and chain the length respectively, ν is the Flory exponent [40–42]. Therefore in the limit solvent viscosity $\eta_s \rightarrow 0$, it has a non-zero intercept proportional to the internal viscosity η_i . This is what exactly seen in recent experiments where the plot of reconfiguration time vs solvent viscosity has a finite intercept equal to the time scale for the internal friction. To the best of our knowledge so far all the theoretical attempts on loop formation in a single chain with internal friction have been restricted to θ solvent, with $\nu = 1/2$, when the chain behaves ideally. But the experimental conditions remain close to a good solvent rather than a θ solvent. There have been few theoretical studies to elucidate the effect of solvent quality on loop formation in single polymer chain [43–45] and unfortunately there exists almost no theoretical study to analyze the combined effect of sol-

vent quality and internal friction on the ring closure dynamics in polymer chains other than the very recent simulation by Yu and Luo [46]. Apart from the solvent quality, denaturant concentration does play an important role in ring closure dynamics [31, 47] of proteins as it profoundly affects the compactness of the protein and routinely used in experiments. Very recently Samanta and Chakrabarti [31] used a compacted Rouse chain model with internal friction to infer the role of denaturant on ring closure dynamics. But the model works only in the θ solvent condition where a phantom Rouse chain description works. Experiments have been performed with proteins away from the θ conditions where excluded volume interactions along with the internal friction play important roles. To take care of excluded volume interactions one has to go beyond phantom chain description but then the many body nature of the problem does not allow an analytical solution. One possibility would be to perform computer simulation as is recently done by Yu and Luo [46]. Other possibility would be to work with a polymer chain where the excluded volume interactions are taken care of at the mean field level. We take the second route and propose a very general model that takes care of solvent quality as well as denaturant in addition to internal friction. We call it “Solvent Dependent Compacted Rouse with Internal Friction (SDCRIF)”. To take care of solvent effect we closely follow the work of Panja and Barkema [48] where an approximate analytical expression for the end to end vector correlation function for a flexible chain in an arbitrary solvent was proposed based on a series of computer simulations. The expression carries a parameter ν similar in the spirit of Flory exponent [40–42, 49, 50] which takes care of solvent quality. A value of $\nu = 1/2$ corresponds to a θ solvent and in that case the correlation function is exact and reduces to the text book expression for the ideal chain [51, 52], on the other hand $\nu = 3/5$ (0.588 more precisely) [48] corresponds to a self avoiding flexible chain (good solvent) as is the case with real polymers. Importantly the same expression can be used for a range of values of ν corresponding to different solvent qualities. Very recently such a mean field Flory exponent based model has been used to describe ring polymer dynamics [53]. Next is the inclusion of internal friction which is done similarly as in case of a phantom polymer chain [54]. Further to take care of the denaturant which controls the compactness of the protein a confining harmonic potential with force constant k_c is used as is done in a very recent study by the authors [31] and also in the context of diffusing polymers in microconfinements [55] or in case of bubble formation in double stranded DNA [56]. So the novelty of SDCRIF remains in its applicability for a range of solvent quality,

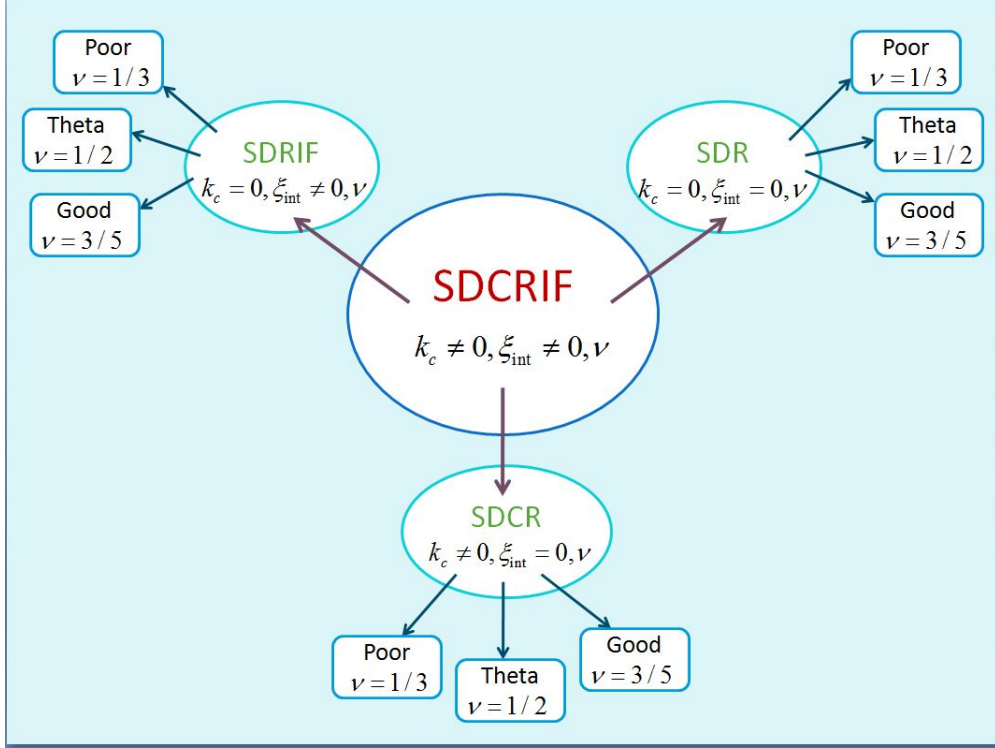


FIG. 1: Solvent Dependent Compacted Rouse with Internal Friction (SDCRIF)

denaturant concentration and in addition it also takes care of internal friction (ξ_{int}) when required. SDCRIF reduces to Rouse model in the limit $\nu = 1/2, k_c = 0, \xi_{int} = 0$ and to “Compacted Rouse with Internal Friction (CRIF)” [30] in the limit $k_c \neq 0, \xi_{int} \neq 0, \nu = 1/2$. The looping dynamics is studied within Wilemski Fixman (WF) framework [13, 57] with SDCRIF, assuming the polymer chain to be Gaussian. It is worth mentioning that WF formalism has extensively been used to calculate the average ring closure or looping time in presence of hydrodynamic interactions by Chakrabarti [58] and to elucidate the effect of viscoelastic solvent [59, 60] and even applied to ring closing of a semiflexible chain [61].

The arrangement of the paper is as follows. The model SDCRIF is introduced in section **II**. Section **III** deals with the method used to calculate the reconfiguration and ring closure time. Results and discussions are presented in section **IV** and section **V** concludes the paper.

II. SOLVENT QUALITY DEPENDENT COMPACTED ROUSE WITH INTERNAL FRICTION (SDCRIF)

In the Rouse model, the polymer chain is treated as a phantom chain [51, 52], where the hydrodynamics interactions and the excluded volume effects are not present. If $R_n(t)$ denotes the position of the n^{th} monomer at time t of such a chain, made of $(N+1)$ monomers, n varying from 0 to N . The equation describing the dynamics of the chain is the following

$$\xi \frac{\partial R_n(t)}{\partial t} = k \frac{\partial^2 R_n(t)}{\partial n^2} + f(n, t) \quad (1)$$

Where ξ denotes the friction coefficient and $k = \frac{3k_B T}{b^2}$ is the spring constant where b is the Kuhn length. $f(n, t)$ is the random force with moments

$$\langle f(n, t) \rangle = 0, \langle f_\alpha(n, t_1) f_\beta(m, t_2) \rangle = 2\xi k_B T \delta_{\alpha\beta} \delta(n - m) \delta(t_1 - t_2) \quad (2)$$

The above equation is solved by decomposing it into normal modes as follows $R_n(t) = X_0 + 2 \sum_{p=1}^{\infty} X_p(t) \cos(\frac{p\pi n}{N})$. In the normal mode description the above force balance equation transforms to the following

$$\xi_p \frac{dX_p(t)}{dt} = -k_p X_p(t) + f_p(t) \quad (3)$$

The time correlation function of the normal modes is

$$\langle X_{p\alpha}(0) X_{q\beta}(t) \rangle = \frac{k_B T}{k_p} \delta_{pq} \delta_{\alpha\beta} \exp(-t/\tau_p) \quad (4)$$

The above expression is for a phantom polymer chain, a chain in θ solvent. In reality θ condition is rarely achieved and the chain behaves as in a good solvent where the chain swells due to the excluded volume interactions. For example Buscaglia et. al showed [47] that to a 11 residue polypeptide chain, 6M GdmCl and 8 M urea are good solvents but aqueous buffer is very close to a θ solvent. It is also not uncommon to encounter a situation representing more of a bad solvent where the chain has a collapsed conformation. To take care of solvent quality we introduce an exponent ν similar in the spirit of Flory exponent [51] in the above expression for the time correlation function of the normal modes. This inclusion closely follows the work of Panja and Barkema [48]. Apart from the solvent quality the presence of denaturant also alters protein conformation. Recently such effects have been

Parameter	SDR	SDRIF	SDCR	SDCRIF
ξ_p	$\xi_p^{SDR} = 2N\xi$	$\xi_p^{SDRIF} = \xi_p^{SDR} + \frac{2\pi^2 p^{2\nu+1} \xi_{int}}{N^{2\nu}}$	$\xi_p^{SDCR} = \xi_p^{SDR}$	$\xi_p^{SDCRIF} = \xi_p^{SDRIF}$
k_p	$k_p^{SDR} = \frac{6\pi^2 k_B T p^{2\nu+1}}{N^{2\nu} b^2}$	$k_p^{SDRIF} = k_p^{SDR}$	$k_p^{SDCR} = 2Nk_c + k_p^{SDR}$	$k_p^{SDCRIF} = 2Nk_c + k_p^{SDR}$
τ_p	$\tau_p^{SDR} = \frac{\xi_p^{SDR}}{k_p^{SDR}} = \frac{\tau^{SDR}}{p^{2\nu+1}}$	$\tau_p^{SDRIF} = \frac{\xi_p^{SDR}}{k_p^{SDRIF}} + \tau_{int}^{SDRIF}$	$\tau_p^{SDCR} = \frac{\xi_p^{SDR}}{k_p^{SDCR}}$	$\tau_p^{SDCRIF} = \frac{\xi_p^{SDR}}{k_p^{SDCRIF}} + \tau_{int}^{SDCRIF}$
τ_{int}	0	$\tau_{int}^{SDRIF} = \frac{\xi_{int}}{k}$	0	$\tau_{int}^{SDCRIF} = \frac{\xi_{int}}{k + k_c N^{2\nu+1} / p^{2\nu+1} \pi^2}$

TABLE I: List of parameters for SDR, SDRIF, SDCR and SDCRIF

taken care of by introducing a confining potential $-\frac{\partial}{\partial R_n}(\frac{k_c}{2}(R_n - 0)^2)$ where, k_c is the spring constant. In addition such a chain can possess what is known as the internal friction, ξ_{int} and can be termed as ‘‘Solvent Dependent Compacted Rouse with Internal Friction (SDCRIF)’’. Earlier works discuss in detail how the inclusion of internal friction is done [29, 54]. Like the Rouse model the end to end distribution of the polymer chain remains Gaussian in SDCRIF as well. Experiments also showed that Gaussian Distributions of end to end distances of proteins are not too bad approximations [11, 62]. Any deviations from the Gaussian behavior is negligibly small [63]. For SDCRIF the basic structure of the correlation function remains the same but has three extra parameters ν , ξ_{int} and k_c .

$$\langle X_{p\alpha}(0)X_{q\beta}(t) \rangle = \frac{k_B T}{k_p^{SDCRIF}} \delta_{pq} \delta_{\alpha\beta} \exp\left(-t/\tau_p^{SDCRIF}\right) \quad (5)$$

Where, $k_p^{SDCRIF} = \frac{6\pi^2 k_B T p^{2\nu+1}}{N^{2\nu} b^2} + 2Nk_c$ and $\xi_p^{SDCRIF} = 2N\xi + \frac{2\pi^2 p^{2\nu+1} \xi_{int}}{N^{2\nu}}$. The relaxation time for p^{th} mode is $\tau_p^{SDCRIF} = \frac{\xi_p^{SDCRIF}}{k_p^{SDCRIF}}$. As expected with $\nu = 1/2$ which corresponds to θ solvent, SDCRIF gives back ‘‘compacted Rouse with internal friction (CRIF)’’ [31], when k_c and ξ_{int} both are nonzero. A more realistic situation would be $\nu = 3/5$ corresponding to good solvent. If the confining potential is removed, the model no longer represents a compacted chain but still remains solvent dependent Rouse and can be termed as ‘‘solvent dependent Rouse with internal friction (SDRIF)’’. Further if the internal friction ξ_{int} is ignored but $\nu \neq 1/2$, the model reduces to solvent dependent Rouse (SDR), and as expected, in the limit when ξ_{int} , k_c both are zero and $\nu = 1/2$, Rouse chain is recovered. Another model would be ‘‘solvent dependent compacted Rouse (SDCR)’’ when $\xi_{int} = 0$, but $k_c \neq 0$. SDCR can account for denaturant effect even in the absence of internal friction which we have used later to reproduce the reconfiguration time of an IDP in high denaturant concentration when internal friction should be negligible. Fig. (1) summarises the models and Table. I depicts all the models along with the parameters describing the models.

III. CALCULATION METHODS

A. Reconfiguration time

The time correlation function of the end-to-end vector is calculated from the correlation of normal modes as follows

$$\phi_{N0}(t) = \langle R_{N0}(0) \cdot R_{N0}(t) \rangle^{SDCRIF} = 16 \sum_{p=1}^{\infty} \frac{3k_B T}{k_p^{SDCRIF}} \exp(-t/\tau_p^{SDCRIF}) \quad (6)$$

Therefore,

$$\phi_{N0}(0) = \langle R_{N0}^2 \rangle_{eq}^{SDCRIF} = 16 \sum_{p=1}^{\infty} \frac{3k_B T}{k_p^{SDCRIF}} \quad (7)$$

The exact expression for $\langle R_{N0}^2 \rangle_{eq}^{SDCRIF}$ is not analytically trackable. However for θ solvent when $\nu = 1/2$, it has an analytical expression [31]

$$\langle R_{N0}^2 \rangle_{eq, \nu=1/2}^{CRIF} = \frac{2b\sqrt{3k_B T}}{\sqrt{k_c}} \tanh\left[\frac{Nb\sqrt{k_c}}{2\sqrt{3k_B T}}\right] \quad (8)$$

Fortunately for SDRIF, $\langle R_{N0}^2 \rangle_{eq}$ has an analytical expression too

$$\langle R_{N0}^2 \rangle_{eq}^{SDRIF} = \frac{2^{2-2\nu}(-1 + 2^{1+2\nu})\zeta[1 + 2\nu]b^2 N^2}{\pi^2} \quad (9)$$

Where, $\zeta[x] = \frac{1}{\Gamma(x)} \int_0^{\infty} \frac{u^{x-1}}{e^u - 1}$ is Riemann Zeta function and $\Gamma(x)$ is the gamma function.

Reconfiguration time τ_{N0} is obtained by integrating the normalized $\phi_{N0}(t)$ [29, 30]

$$\tau_{N0} = \int_0^{\infty} dt \tilde{\phi}_{N0}(t) \quad (10)$$

Where, $\tilde{\phi}_{N0}(t) = \frac{\phi_{N0}(t)}{\phi_{N0}(0)}$

B. Looping time

Wilemski Fixman (WF) approach is a widely accepted method to calculate the time required to form a loop between two parts of a Gaussian polymer chain [13]. This formalism gives the following expression for the looping time between two ends of the chain.

$$\tau_{N0}^{loop} = \int_0^{\infty} dt \left(\frac{C_{N0}(t)}{C_{N0}(\infty)} - 1 \right) \quad (11)$$

Where, $C_{N_0}(t)$ is the sink-sink correlation function given by

$$C_{N_0}(t) = \int dR_{N_0} \int dR_{N_0,0} S(R_{N_0}) G(R_{N_0}, t | R_{N_0,0}, 0) S(R_{N_0,0}) P(R_{N_0,0}) \quad (12)$$

$G(R_{N_0}, t | R_{N_0,0}, 0)$ is the conditional probability of the polymer to have end-to-end distance R_{N_0} at time t , which was $R_{N_0,0}$ at time $t = 0$.

$$G(R_{N_0}, t | R_{N_0,0}, 0) = \left(\frac{3}{2\pi \langle R_{N_0}^2 \rangle_{eq}^{SDCRIF}} \right)^{3/2} \left(\frac{1}{(1 - \tilde{\phi}_{N_0}^2(t))^{3/2}} \right) \exp \left[-\frac{3(R_{N_0} - \tilde{\phi}_{N_0}(t)R_{N_0,0})^2}{2 \langle R_{N_0}^2 \rangle_{eq}^{SDCRIF} (1 - \tilde{\phi}_{N_0}^2(t))} \right] \quad (13)$$

When the sink function $S(R_{mn})$ [64–66] is chosen to be a delta function then the looping time of SDCRIF has the following expression [67]

$$\tau_{N_0}^{loop,SDCRIF} = \int_0^\infty dt \left(\frac{\exp[-2\chi_0 \tilde{\phi}_{N_0}^2(t)/(1 - \tilde{\phi}_{N_0}^2(t))] \sinh[(2\chi_0 \tilde{\phi}_{N_0}(t))/(1 - \tilde{\phi}_{N_0}^2(t))] - 1}{(2\chi_0 \tilde{\phi}_{N_0}(t)) \sqrt{1 - \tilde{\phi}_{N_0}^2(t)}} \right) \quad (14)$$

Where,

$$\chi_0 = \frac{3a^2}{2 \langle R_{N_0}^2 \rangle_{eq}^{SDCRIF}} \quad (15)$$

IV. RESULTS

A. Equilibrium end to end distribution

The equilibrium distribution of the vector connecting end-to-end monomers of a Gaussian chain is given by $P(R_{N_0}) = \left(\frac{3}{2\pi \langle R_{N_0}^2 \rangle} \right)^{3/2} \exp \left[-\frac{3R_{N_0}^2}{2 \langle R_{N_0}^2 \rangle} \right]$, where, $\langle R_{N_0}^2 \rangle$ denotes the average equilibrium end to end distance of the polymer. This expression holds for SDCRIF as well since the model is considered to be Gaussian in our description. In Fig. (2) the equilibrium distribution of the end-to-end distance is shown for the polymer at different solvent quality in absence of the confining potential. As expected the distribution plot is broader for the polymer in good solvent ($\nu = 3/5$) in comparison to the polymer in poor solvent ($\nu = 1/3$). From good to θ to bad solvent the most probable end to end distance or the peak position shifts to lower value as a signature of swelled to collapsed transition.

The parameters have been chosen in accordance to the work by Schuler's group [11] on cold shock protein (Csp) and prothymosin α (ProT α) and has been mentioned in all the figures. In Fig. (3) the same distribution is shown for good solvent but in presence of three different values of k_c . As the k_c controls the compactness of the polymer, increasing the value of k_c should result in the higher degree of internal friction. Since there is no first principle relation between k_c and ξ_{int} , we have used an ansatz in our calculation [12, 31]. The ansatz connects k_c with ξ_{int} as follows $k_c = \tilde{k}_c + k_{c,0}(c_0 + c_1 n_b + c_2 n_b^2 + \dots)$, where, $k_{c,0} = A \frac{\xi_{int,0}}{\tau_{int,0}}$, and $\xi_{int} = \xi_{int,0}(c_0 + c_1 n_b + c_2 n_b^2 + \dots)$. $\xi_{int,0}$ is the zeroth order approximation to internal friction which only accounts for the interactions between a monomer with its two nearest neighbours, $\tau_{int,0}$ is the corresponding time scale, n_b is the number of non-adjacent monomers contributing to the internal friction and A is considered typically in the order of $\pi^2/N^{2\nu+1}$ whereas other parameters are constants with no or very weak dependence on chain properties. Therefore k_c has a part proportional to $\xi_{int,0}$. However, in the limit $\xi_{int,0} = 0$, $k_c = \tilde{k}_c$. If the value of k_c or the strength of the confinement increases the end to end distance probability distribution becomes narrower, a sign of more compacted polymer chain. This can clearly be seen from the plot of end to end distance distribution at different values of k_c depicted in Fig. (3). Thus k_c and ν plays significant roles in deciding the width and height of the end to end distribution. But the the parameters have different physical significance and play different roles in the chain dynamics. The exponent ν takes care of the quality of the solvent around the chain and has no dependence on ξ_{int} and no or very weak dependence on denaturant concentration [47]. But k_c on the other hand takes care the effect of the denaturant on the chain and has ξ_{int} dependence as well. Here we also attempt to make a qualitative comparison of our model SDCRIF with the very recent simulation from Luo's [46] group. Fig. 3. of [46], shows similar trend of the end to end probability distribution on changing the parameter λ , a measure of attractive interaction between the beads. Higher the value of λ poorer the solvent, narrower the distribution.

B. Relaxation time for the Normal modes

In order to calculate reconfiguration time one has to calculate the correlation function between normal modes defined in Eq. 5. The functional form of τ_p^{SDCRIF} is given in Table. I. The lower normal modes contribute largely to looping and reconfiguration dynamics [57]. A

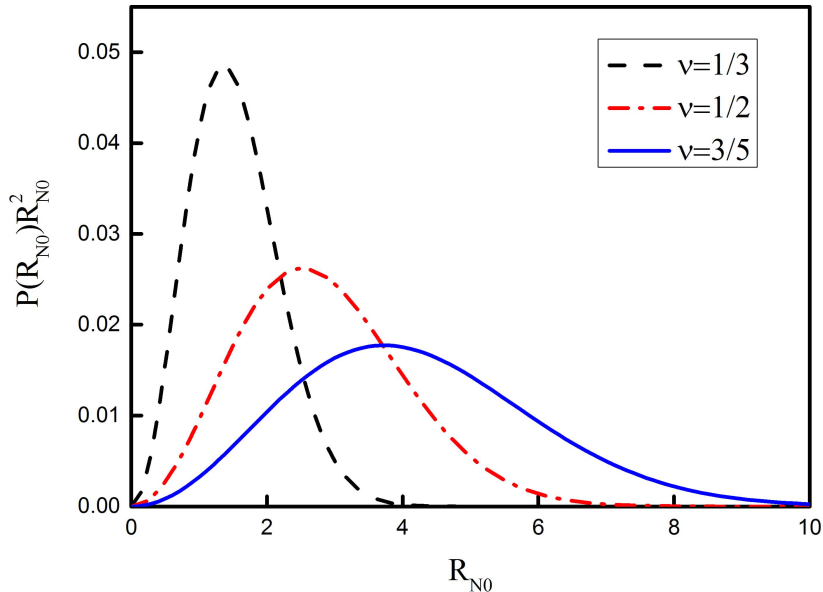


FIG. 2: End-to-end distribution at different solvent quality with $k_c = 0$. The values of parameters used are $N = 66$, $b = 3.8 \times 10^{-10}m$, $\xi = 9.42 \times 10^{-12}kg s^{-1}$, $k_B = 1.38 \times 10^{-23}JK^{-1}$ and $T = 300K$.

plot of τ_p^{SDCRIF} vs ν for the first normal mode is shown in Fig. (4). This shows how τ_p^{SDCRIF} changes with the solvent quality if all the other parameters remain fixed. The plot shows that τ_p^{SDCRIF} (for $p = 1$) increases with ν . Thus for poor solvents corresponding to lower value of ν , τ_p^{SDCRIF} is lower and as one approaches good solvent τ_p^{SDCRIF} increases resulting in slower relaxation. This would definitely lead to slower reconfiguration and looping time in good solvent as compared to bad or poor solvent. Similar trend for the third normal mode can be seen from the plot in the inset of the Fig. (4). Recent simulation also confirm this [46] and shows an order of magnitude increase in the looping time in the good solvent as compared to the poor solvent. The reconfiguration times of a chain for different values of ν are shown in Fig. (5). It can be seen that at a value $\eta/\eta_0 = 1$, the reconfiguration time increases by a factor of 6 on changing $\nu = 1/3$ to $\nu = 3/5$.

C. Solvent viscosity dependence

One aspect of the reconfiguration time is its dependence on solvent viscosity [29]. Experiments show a linear dependence of reconfiguration time on solvent viscosity [11]. In Fig. (5)

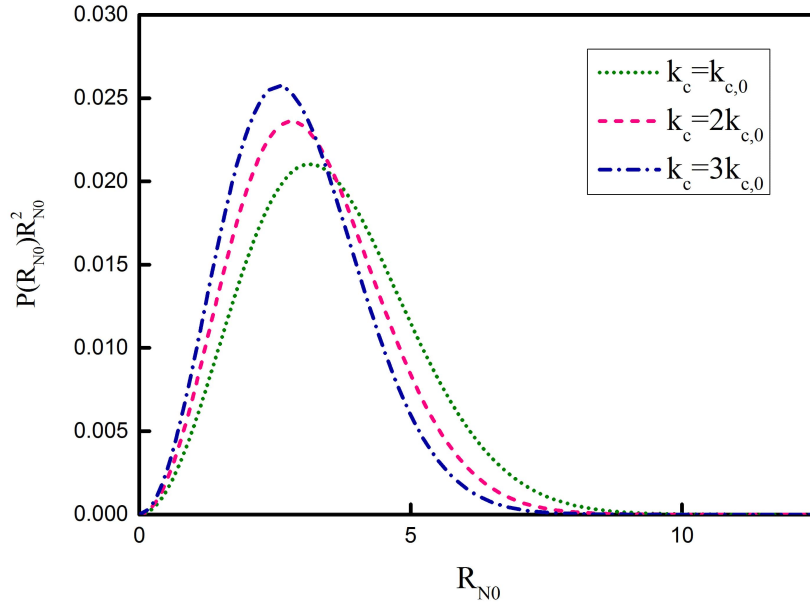


FIG. 3: End-to-end distribution at different values of k_c for good solvent ($\nu = 3/5$). The values of parameters used are $N = 66$, $\tilde{k}_c = 0$, $b = 3.8 \times 10^{-10}m$, $\xi = 9.42 \times 10^{-12}kg s^{-1}$, $k_B = 1.38 \times 10^{-23}JK^{-1}$ and $T = 300K$.

the reconfiguration times ($\tau_{N_0}^{SDRIF}$) are plotted against the solvent viscosity at different values of ν in absence of any confining potential ($k_c = 0$) and non zero internal friction ($\xi_{int} \neq 0$). The figure clearly shows $\tau_{N_0}^{SDRIF}$ increases linearly with increasing normalized solvent viscosity η/η_0 , with a positive intercept in the limit $\eta/\eta_0 \rightarrow 0$, η_0 being the viscosity of water. What is surprising is the value of intercept is practically independent of solvent quality. This intercept corresponds to the internal friction which is completely dry in this case. The trend can be fitted with an almost analytically exact expression $\tau_{N_0}^{SDR} \simeq \tau_{int}^{SDR} + C(\nu)\tau^{SDR}$, where $\tau^{SDR} = \frac{\xi N^{2\nu+1} b^2}{3\pi^2 k_B T}$ and $C(\nu)$ s have ν dependence and are 0.73, 0.82 and 0.87 for the poor, θ and good solvent respectively. Thus poorer the solvent lower the slope. In poor solvent reconfiguration time is not only fast but also less affected by the viscosity of the solvent. This is presumably because of the collapsed form of the polymer chain. Fig. (6) is the plot of $\tau_{N_0}^{SDCRIF}$ vs η/η_0 in presence of a fixed confining potential $k_{c,0}$ but at three different values of ν covering a range of solvent qualities. Interestingly in this case the intercepts are found to be different when the intercepts were magnified as can be seen in the inset of Fig. (6). This is because τ_{int}^{SDCRIF} has k_c as well as ν dependence as can be seen from the Table. I. So even

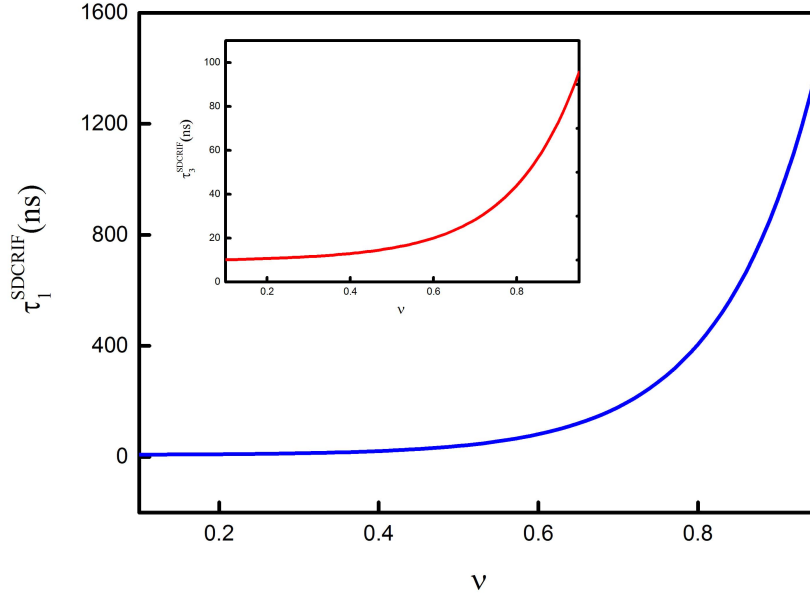


FIG. 4: τ_p^{SDCRIF} vs ν for $p = 1$ and $p = 3$ (inset). The values of parameters used are $N = 66$, $k_c = k_{c,0}$, $\tilde{k}_c = 0$, $b = 3.8 \times 10^{-10}m$, $\xi = 9.42 \times 10^{-12}kgs^{-1}$, $\xi_{int,0} = 100 \times \xi$, $k_B = 1.38 \times 10^{-23}JK^{-1}$ and $T = 300K$.

with the same value of k_c , changing ν would result a change in the effective force constant, $k_{eff} \simeq k + k_c N^{2\nu+1} / \pi^2 p^{2\nu+1}$ of the chain and hence a change in the value of the intercept. In all the cases ξ_{int} remains the same and the time scales associated with the internal friction τ_{int}^{SDCRIF} are changed by very small amount which means the dependence of τ_{int}^{SDCRIF} on ν is very weak and it cannot reproduce the denaturant effect observed in the experiments, which is why we need k_c and the ansatz which connects k_c with ξ_{int} to take care of the denaturant effect on a polymer without changing the solvent quality. This can be seen in Fig. (7) where we have looked into the viscosity dependence of τ_{N0}^{SDCRIF} in different values of k_c for good solvent ($\nu = 3/5$). In this case the change in the values of the intercepts is very evident because of the different degrees of compactness of the chain. Another important observation is the case with higher k_c value has a higher intercept but it is less steeper making the change in the reconfiguration time less prone to the viscosity of the solvent. This is how k_c can replicate the experimental results [11] where it has been found that if denaturant is introduced to a polymer solution, the polymer becomes less compact which results in lower value of internal friction ξ_{int} . k_c controls the compactness of the protein thus connects to the

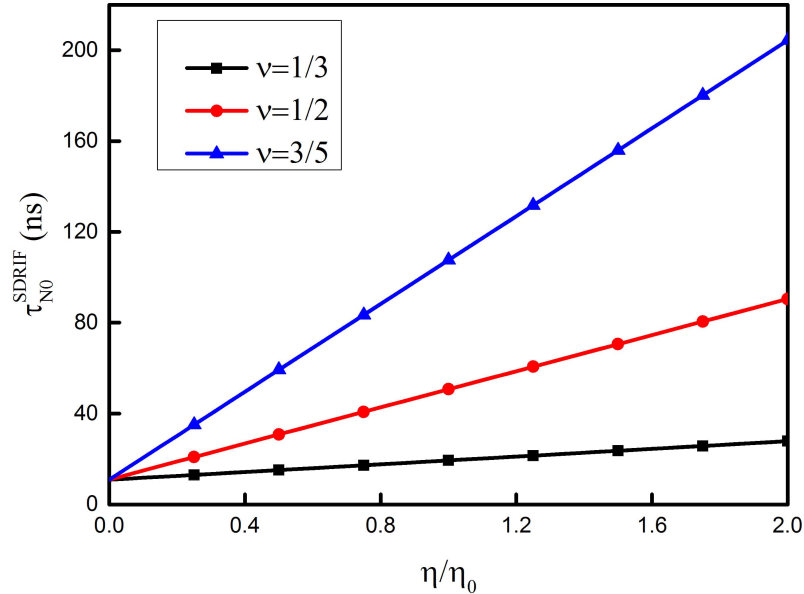


FIG. 5: Reconfiguration time (τ_{N0}^{SDRIF}) vs solvent viscosity at different solvent quality. The values of parameters used are $N = 66$, $k_c = 0$, $b = 3.8 \times 10^{-10}m$, $\xi = 9.42 \times 10^{-12}kgs^{-1}$, $\xi_{int,0} = 100 \times \xi$, $k_B = 1.38 \times 10^{-23}JK^{-1}$ and $T = 300K$.

denaturant concentration. The higher the denaturant concentration lower the k_c value. This is also reflected in our ansatz as increasing denaturant concentration would mean smaller n_b and lower internal friction ξ_{int} . But k_c does not speak for the solvent quality rather it is ν which accounts for that. In the later section we used SDCRIF to compare experimental data on cold shock protein and prothymosin α (ProT α) [11] and have confirmed this. We have also looked at the viscosity dependence of the looping time and have found it to be $\sim \eta^\beta$ with $\beta < 2$ [29, 68]. A detailed study on the viscosity dependence of the looping time can be found in one of our earlier works [29].

D. Chain length dependence

Fig. (8) is the log-log plot of the reconfiguration time for a chain with $k_c = 0$, $\xi_{int} = 0$ vs chain length N of the polymer for different values of ν , the parameter accounting for the solvent quality. There is a general trend, $\tau_{N0}^{SDR} \sim N^{2\nu+1}$ as $\tau_{N0}^{SDR} = C(\nu)\tau^{SDR}$. This result is expected and can be predicted by looking at the scaling of the end to end vector correlation

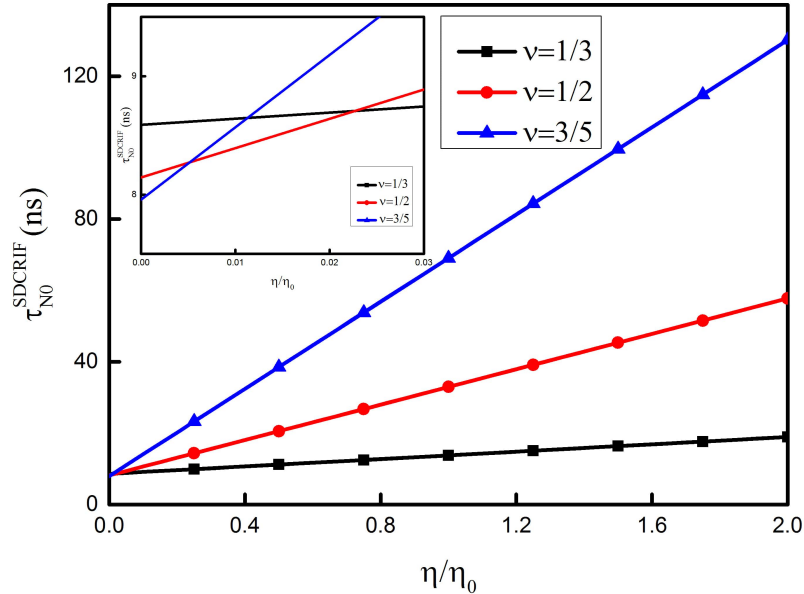


FIG. 6: Reconfiguration time (τ_{N0}^{SDCRIF}) vs solvent viscosity at different solvent quality. The values of parameters used are $N = 66$, $k_c = k_{c,0}$, $\tilde{k}_c = 0$, $b = 3.8 \times 10^{-10}m$, $\xi = 9.42 \times 10^{-12}kg s^{-1}$, $\xi_{int,0} = 100 \times \xi$, $k_B = 1.38 \times 10^{-23}JK^{-1}$ and $T = 300K$.

function with the chain length. When the same calculations were done in presence of internal friction as shown in Fig. (9) the dependence on the chain length becomes weaker in general but the relative trend remains the same, in poor solvent dynamics is faster. Although the chain reconfiguration in general become slower due to the presence of internal friction. To see how the chain dynamics changes in presence of the confining potential the same calculations were again performed for three different values of k_c but putting internal friction $\xi_{int} = 0$ in good solvent ($\nu = 3/5$) as shown in Fig. (10). Here as $\xi_{int} = 0$ therefore, $k_{c,0} = 0$ and $k_c = \tilde{k}_c$ whereas \tilde{k}_c is scaled as $k_{c,0}$. This result is very interesting as it can be seen from the Fig. (10), that the N dependence remains practically unchanged. The reason for this as follows. We restrict ourselves to a value of k_c such that the effective force constant $k_{eff} \simeq k + k_c N^{2\nu+1} / \pi^2 p^{2\nu+1}$ is in the same order of magnitude of k . For example a choice of $k_c \simeq k \pi^2 / N^{2\nu+1}$ gives $k_{eff} \simeq k(1 + p^{2\nu+1})$. Now since lower normal modes contribute mostly in reconfiguration dynamics [57], taking the contribution from $p = 1$ normal mode gives $k_{eff} \simeq 2k$ and thus leads to unchanged scaling of the reconfiguration time with the

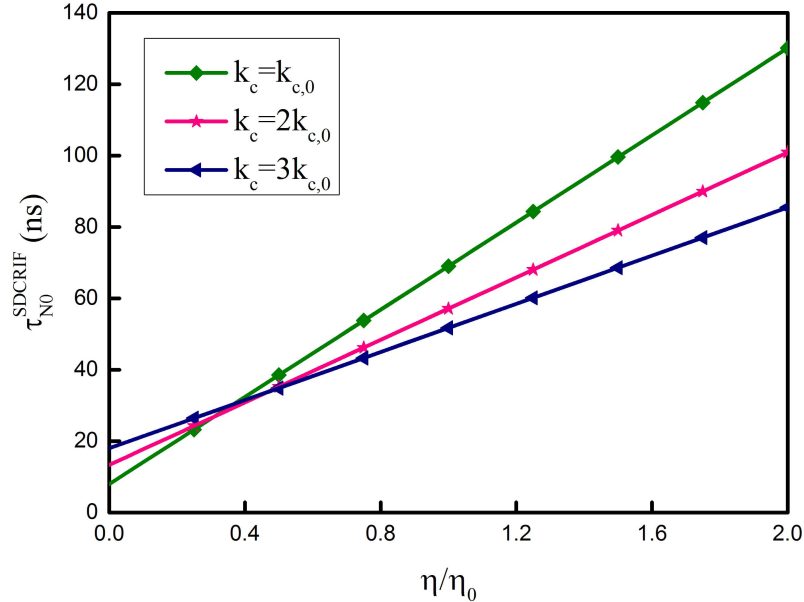


FIG. 7: Reconfiguration time (τ_{N0}^{SDCRIF}) vs solvent viscosity at different values of k_c for good solvent ($\nu = 3/5$). The values of parameters used are $N = 66$, $\tilde{k}_c = 0$, $b = 3.8 \times 10^{-10}m$, $\xi = 9.42 \times 10^{-12}kgs^{-1}$, $k_B = 1.38 \times 10^{-23}JK^{-1}$ and $T = 300K$.

chain length N for a given value of ν . Similar calculations have been done for looping time based on the WF approximation [13] as can be seen from Fig. (11) and Fig. (12). The same arguments hold for the looping time and the trends are similar. Scaling of the looping time as N^2 for the Rouse chain [58, 69] as obtained earlier can be confirmed with a choice of $\nu = 1/2$, $k_c = 0$ and $\xi_{int} = 0$ and is shown in Fig. (11).

E. Comparison with experiments

In this section we use SDCRIF to compute the reconfiguration time and compare it with the one measured in the recent Förster resonance energy transfer (FRET), nanosecond fluorescence correlation spectroscopy and microfluidic mixing based study on cold shock protein from *Thermotoga maritima* (Csp) labeled at positions 2 and 68 with Alexa 488 and Alexa 594 as donor and acceptor, respectively [11, 70]. Thus it can be approximated that the labelling are at the two ends of the protein. Their study revealed important role of internal friction in unfolded small cold shock protein and confirmed a time scale of about $\sim 5 - 50$

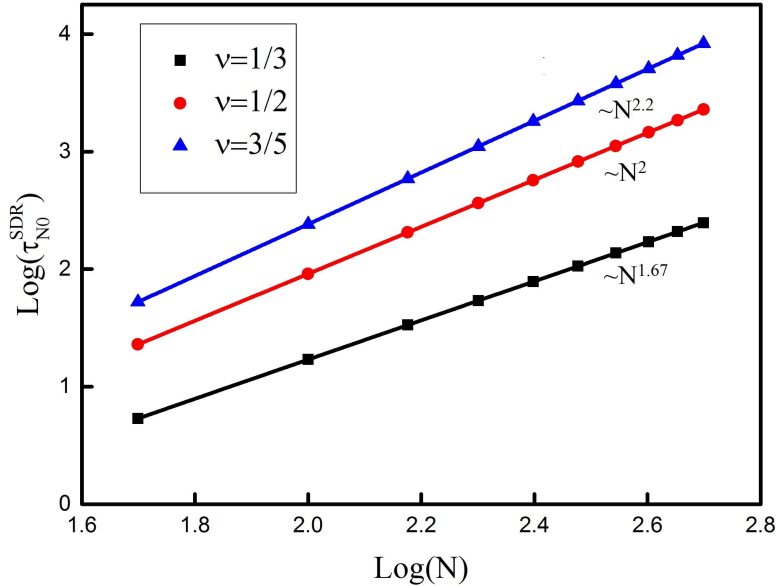


FIG. 8: $\text{Log}(\tau_{N0}^{SDR})$ vs $\text{Log}(N)$ at different solvent quality. The values of parameters used are $k_c = 0$, $b = 3.8 \times 10^{-10}m$, $\xi = 9.42 \times 10^{-12}kg s^{-1}$, $k_B = 1.38 \times 10^{-23}JK^{-1}$, $\xi_{int} = 0$ and $T = 300K$.

ns for the internal friction. Moreover they found the internal friction to strongly depend on the denaturant concentration. Nuclear magnetic resonance and laser photolysis methods also have confirmed the effects of denaturants by showing the rate of intrachain contact formation in unfolded state of carbonmonoxide-liganded cytochrome c (cyt-CO) to increase with increase in denaturant concentration [12]. Higher the denaturant concentration lower the internal friction. On the other hand for an intrinsically disordered protein (IDP) such as C-terminal segment of human prothymosin α (ProT α) magnitude of internal friction is smaller [71, 72] and at high denaturant concentration it is negligibly small. This is presumably due to exposed hydrophilic and charged residues resulting expansion of the protein. But in native buffer the time scale for internal friction is ~ 6 ns which on addition of excess salt like KCl shows ~ 3 times increase in internal friction due to the collapse of the IDP. For both the cases the reconfiguration time measured has a linear dependence on solvent viscosity with an intercept equal to the time scale for the internal friction. Fig. (13) and Fig. (14) show the experimental data and our calculation based on SDCRIF of Csp and ProT α respectively. All the calculations are performed with $\nu = 3/5$, value corresponding to good solvent, which is particularly valid for IDPs. On the other hand, the parameter

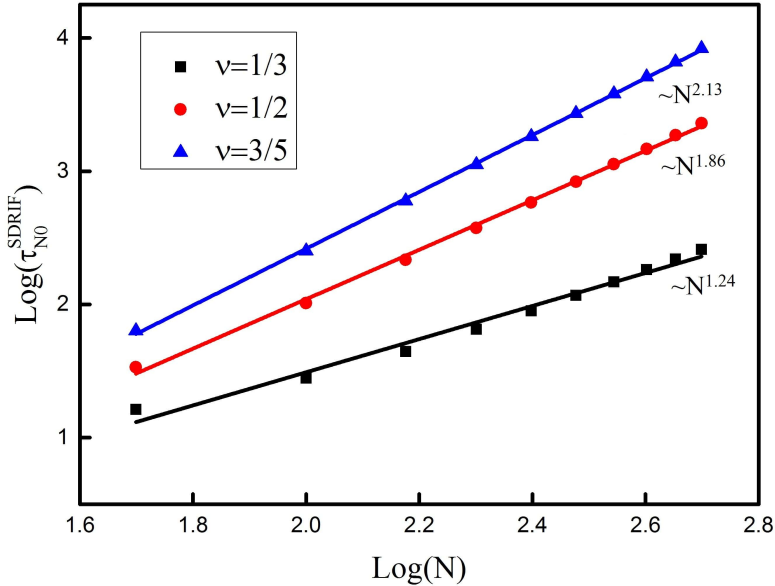


FIG. 9: $\text{Log}(\tau_{N0}^{SDRIF})$ vs $\text{Log}(N)$ at different solvent quality. The values of parameters used are $k_c = 0$, $b = 3.8 \times 10^{-10}m$, $\xi = 9.42 \times 10^{-12}kgs^{-1}$, $\xi_{int,0} = 100 \times \xi$, $k_B = 1.38 \times 10^{-23}JK^{-1}$ and $T = 300K$.

k_c in our model takes care of changes associated with the denaturant concentration and ξ_{int} is the corresponding internal friction which is considered to be zero for the ProT α in high denaturant condition (6MGdmCl) when time scale associated with internal friction was found to be negligible experimentally. In this case $k_c = \tilde{k}_c$ and \tilde{k}_c is scaled as $5.5k_{c,0}$. Table. II and Table. III depict the parameters used in our calculation and show the theoretically calculated internal friction time scales are in excellent quantitative agreement with that measured experimentally.

V. CONCLUSIONS

Motivated by recent experiments [11] on cold shock proteins and intrinsically disordered proteins (IDPs) we have analyzed the effects of denaturant and the solvent quality on the reconfiguration and looping dynamics of a chain with internal friction by using an extended Rouse chain model with internal friction. The model termed as ‘‘Solvent Dependent Compacted Rouse Chain (SDCRIF)’’ takes care of solvent quality through a Flory type exponent

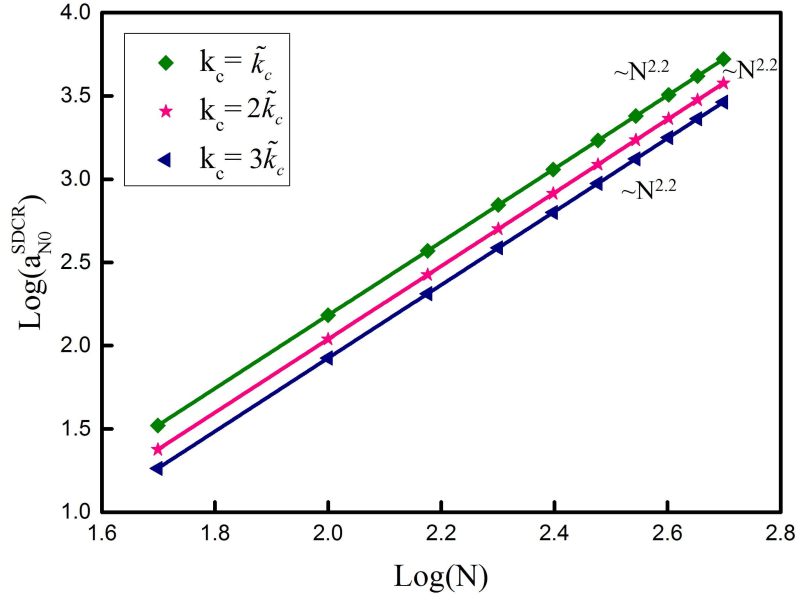


FIG. 10: $\text{Log}(\tau_{N0}^{SDRCRIF})$ vs $\text{Log}(N)$ at different values of k_c for good solvent ($\nu = 3/5$). The values of parameters used are $b = 3.8 \times 10^{-10}m$, $\xi = 9.42 \times 10^{-12}kgs^{-1}$, $\xi_{int,0} = 0$, $k_B = 1.38 \times 10^{-23}JK^{-1}$ and $T = 300K$.

ν and the effects of denaturant concentration are taken care by the strength of a harmonic confinement k_c of the chain. Following an ansatz we further relate k_c with the internal friction. This assures a non zero intercept in the plot of reconfiguration time vs solvent viscosity as found in experiments [11, 50] and also makes it denaturant concentration dependent. Here we would like to point out that mere ‘‘Compacted Rouse with Internal Friction (CRIF)’’ [11, 31] can not convincingly account for the changes in reconfiguration time due to change in solvent quality and for this we need a parameter ν . Also the parameter k_c should be coupled strongly with the internal friction ξ_{int} and this is done through the ansatz mentioned in the result section. For folded protein like cold shock protein the magnitude of the internal friction is high and our theory also reproduce this with a choice of high value of k_c and ξ_{int} . Values of these parameters also change on changing the denaturant concentration. Typically the value of the number of monomers contributing to internal friction, n_b also increases as the denaturant concentration decreases and the protein collapses which demands a higher magnitude of k_c to be used to reproduce the experimental data. On the other hand for the intrinsically disordered protein prothymosin α (ProT α) magnitude of

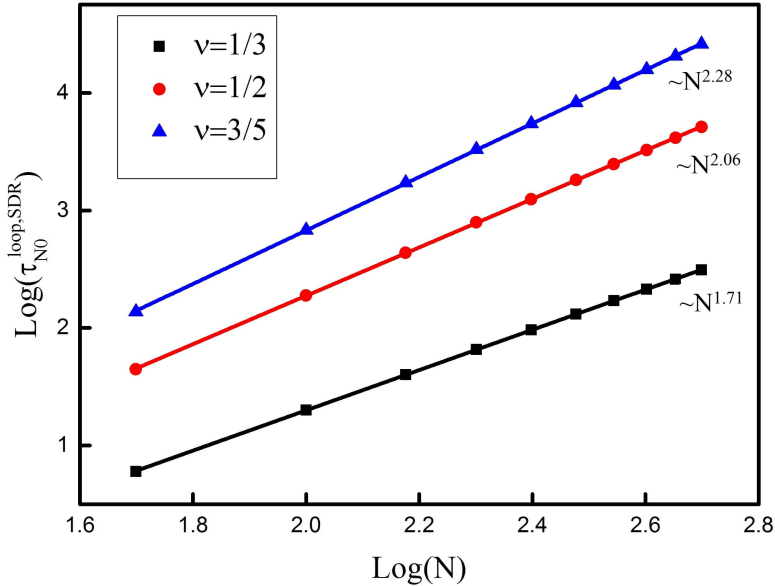


FIG. 11: $Log(\tau_{N0}^{loop,SDR})$ vs $Log(N)$ at different solvent quality. The values of parameters used are $k_c = 0$, $b = 3.8 \times 10^{-10}m$, $\xi = 9.42 \times 10^{-12}kgs^{-1}$, $\xi_{int,0} = 0$, $k_B = 1.38 \times 10^{-23}JK^{-1}$ and $T = 300K$.

k_c and the internal friction ξ_{int} are low. Only in presence of a salt the protein collapses and then a higher magnitude of k_c can reproduce the experimental data. This highlights the novelty of our model which is applicable to a wide range of denaturant concentration, solvent quality and protein types. Whereas k_c in our model effectively renormalizes the force constant of the chain, ν on the other hand takes care of the quality of the solvent around. Both the parameters are essential to explain the experimental data on reconfiguration times of proteins, so as the azsatz that relates k_c with the internal friction ξ_{int} of the chain. Another issue is the relative dependence of the reconfiguration and looping time on ξ_{int} and ν . For the range of values of ξ_{int} we have used throughout our calculation the reconfiguration time (so as the looping time, not shown) depends only weakly on internal friction ξ_{int} and rather strongly on the solvent quality, i.e. ν . This can be seen in Fig. (15) (where $c(\nu)$ is taken to be 0.80 for simplicity) but on increasing the internal friction magnitude by two orders of magnitude the change due internal friction become visible. For example if the ξ_{int} is taken to be 3000ξ for poor solvent ($\nu = 1/3$) the time scale for internal friction become (~ 340 ns) which is ~ 3 times higher than the same (~ 100 ns) in good solvent ($\nu = 3/5$) for

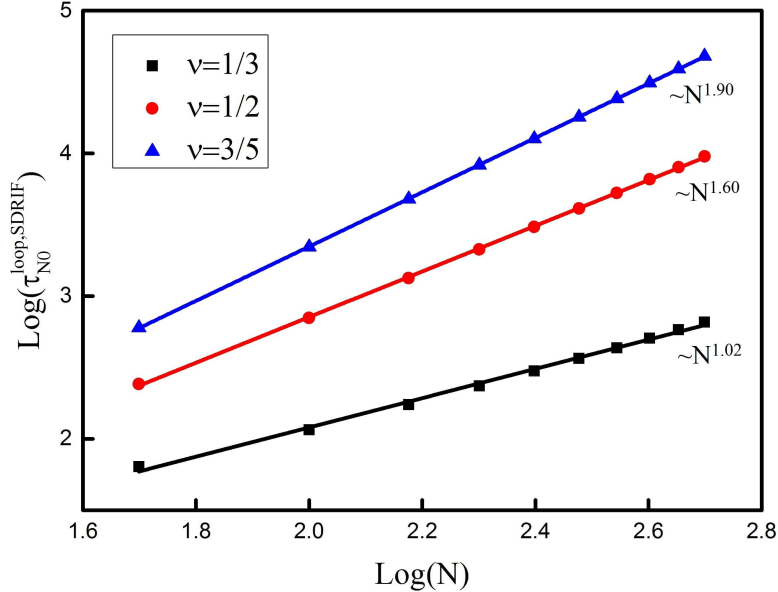


FIG. 12: $\text{Log}(\tau_{N0}^{loop,SDRIF})$ vs $\text{Log}(N)$ at different solvent quality. The values of parameters used are $k_c = 0$, $b = 3.8 \times 10^{-10}m$, $\xi = 9.42 \times 10^{-12}kgs^{-1}$, $\xi_{int,0} = 100 \times \xi$, $k_B = 1.38 \times 10^{-23}JK^{-1}$ and $T = 300K$.

$\xi_{int} = 100\xi$. This is in the same spirit as seen in recent simulation [46], where the looping time passes through a minima while plotted against the parameter λ , a combined measure of solvent quality and internal friction.

We would like to conclude by pointing out that in reality internal friction has contributions from hydrogen bonding, other weak forces and specially torsion angle rotations in proteins and have already been investigated in atomistic simulations [35–37]. Taking these contributions explicitly beyond the scope of this study. However it would be worth incorporating internal friction in a model of polymer with torsion and semiflexibility [52] and explore the physics involved. Work along this direction is under progress.

VI. ACKNOWLEDGEMENT

Authors thank IRCC IIT Bombay (Project Code: 12IRCCSG046), DST (Project No. SB/SI/PC-55/2013) and CSIR (Project No. 01(2781)/14/EMR-II) for funding generously.

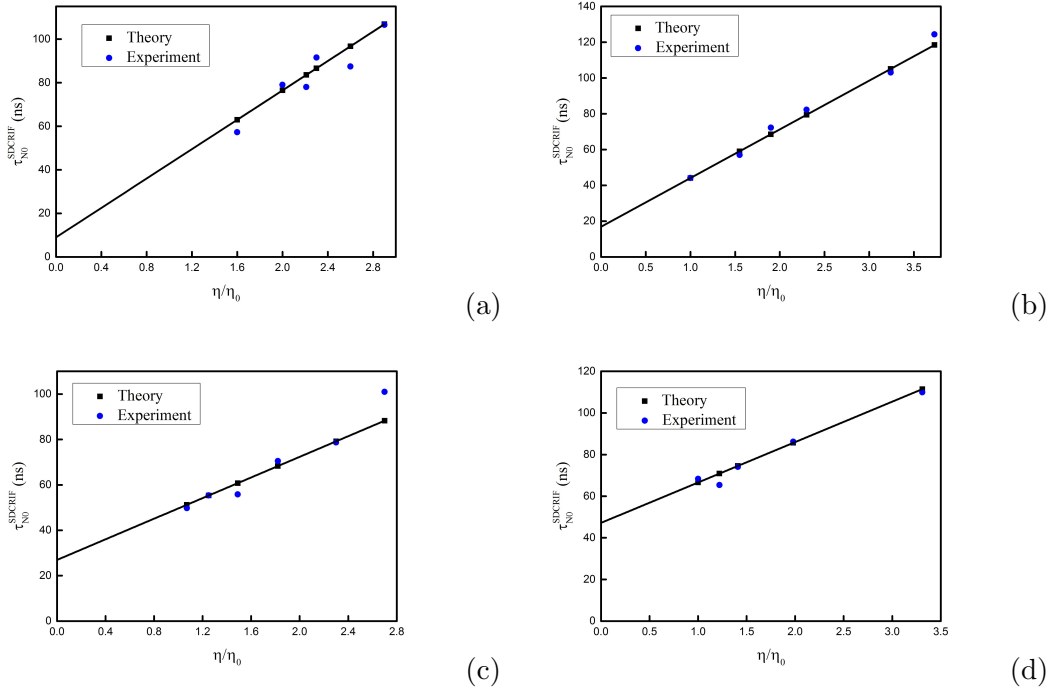


FIG. 13: Comparison between theoretical and experimental reconfiguration time vs solvent viscosity data for the cold shock protein (Csp). (a) 1.3M GdmCl, (b) 2M GdmCl, (c) 4M GdmCl and (d) 6M GdmCl. The values of parameters used are $N = 66$, $\tilde{k}_c = 0$, $b = 3.8 \times 10^{-10}m$, $\xi = 9.42 \times 10^{-12}kgs^{-1}$, $\xi_{int,0} = 100 \times \xi$, $k_B = 1.38 \times 10^{-23}JK^{-1}$ and $T = 300K$.

Denaturant concentration	k_c	ξ_{int}	$\tau_{int}(\text{Theory})$	$\tau_{int}(\text{Experiment})$
1.3M GdmCl	$3.0k_{c,0}$	$9.0\xi_{int,0}$	~ 47 ns	~ 42 ns
2.0M GdmCl	$2.5k_{c,0}$	$5.0\xi_{int,0}$	~ 27 ns	~ 25 ns
4.0M GdmCl	$2.0k_{c,0}$	$3.0\xi_{int,0}$	~ 17 ns	~ 12 ns
6.0M GdmCl	$1.5k_{c,0}$	$1.5\xi_{int,0}$	~ 9 ns	~ 5 ns

TABLE II: Comparison with experimental data on cold shock protein: The values of parameters used are $N = 66$, $\tilde{k}_c = 0$, $b = 3.8 \times 10^{-10}m$, $\xi = 9.42 \times 10^{-12}kgs^{-1}$, $\xi_{int,0} = 100 \times \xi$, $k_B = 1.38 \times 10^{-23}JK^{-1}$ and $T = 300K$.

[1] Y. Rabin and H. C. Öttinger, *Europhys. Lett.* **13**, 423 (1990).

[2] J. D. Schieber, *J. Rheol.* **37**, 1003 (1993).

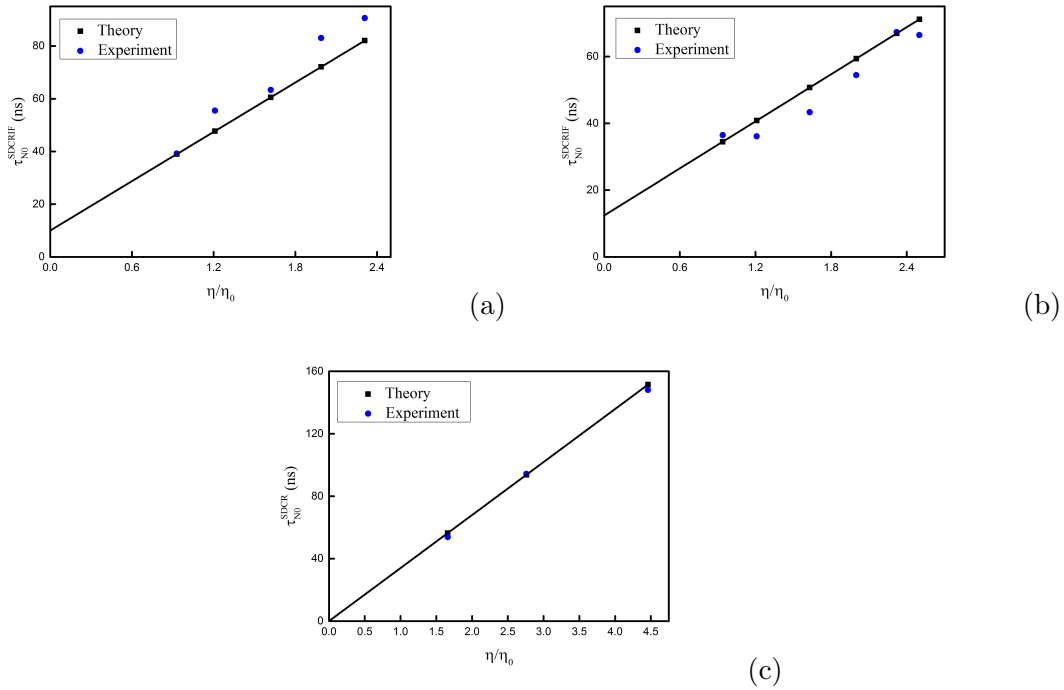
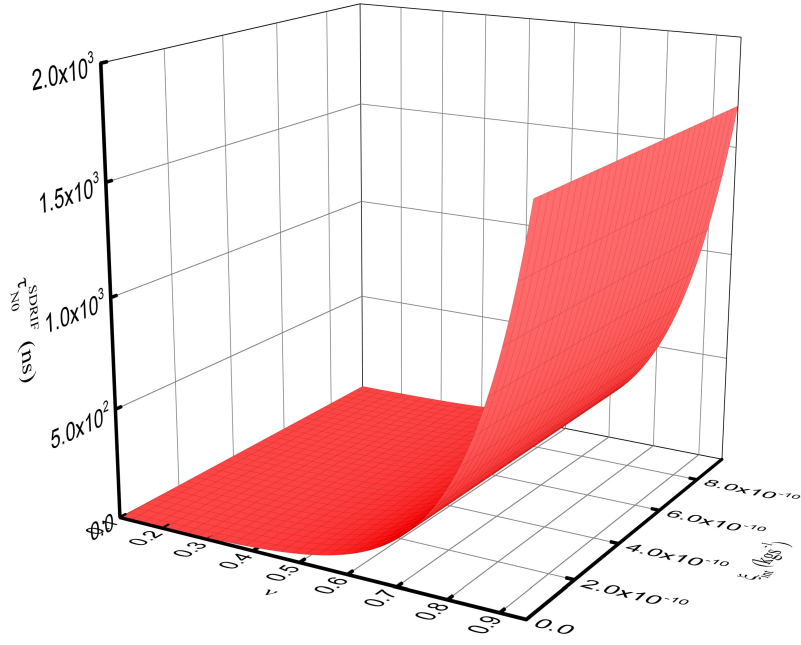


FIG. 14: Comparison between theoretical and experimental reconfiguration time vs solvent viscosity data for IDP ProT α . (a) native buffer, (b) 1M KCl and (b) 6M GdmCl. The values of parameters used are $N = 110$, $b = 3.8 \times 10^{-10}m$, $\xi = 9.42 \times 10^{-12}kgs^{-1}$, $\xi_{int,0} = 100 \times \xi$, $k_B = 1.38 \times 10^{-23}JK^{-1}$ and $T = 300K$.

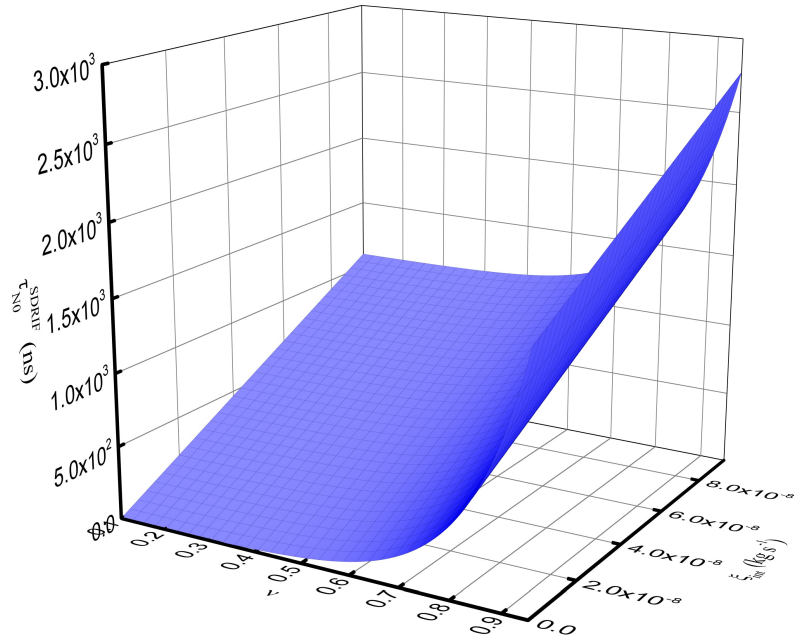
Solvent condition	k_c	ξ_{int}	τ_{int} (Theory)	τ_{int} (Experiment)
Native buffer	$\tilde{k}_c = 0, 6k_{c,0}$	$2.0\xi_{int,0}$	~ 10 ns	~ 6 ns
1M KCl	$\tilde{k}_c = 0, 8k_{c,0}$	$2.5\xi_{int,0}$	~ 12 ns	~ 16 ns
6M GdmCl	$\tilde{k}_c \neq 0, k_{c,0} = 0$	0	0	0

TABLE III: Comparison with experimental data on IDP ProT α : The values of parameters used are $N = 110$, $b = 3.8 \times 10^{-10}m$, $\xi = 9.42 \times 10^{-12}kgs^{-1}$, $\xi_{int,0} = 100 \times \xi$, $k_B = 1.38 \times 10^{-23}JK^{-1}$ and $T = 300K$.

- [3] J. D. Schieber, J. Non-Newtonian Fluid Mech. **45**, 47 (1992).
- [4] C. W. Manke and M. C. Williams, Macromolecules **18**, 2045 (1985).
- [5] D. E. Sagnella, J. E. Straub, and D. Thirumalai, J. Chem. Phys. **113**, 7702 (2000).
- [6] J. J. Portman, S. Takada, and P. G. Wolynes, J. Chem. Phys. **114**, 5082 (2001).
- [7] S. A. Pabit, H. Roder, and S. J. Hagen, Biochemistry **43**, 12532 (2004).



(a)



(b)

FIG. 15: 3D Plot of reconfiguration time vs ν and ξ_{int} . (a) ξ_{int} upto $10^2 \times \xi$, (b) ξ_{int} upto $10^4 \times \xi$. The values of parameters used are $N = 66$, $k_c = 0$, $b = 3.8 \times 10^{-10}m$, $\xi = 9.42 \times 10^{-12}kgs^{-1}$, $k_B = 1.38 \times 10^{-23}JK^{-1}$ and $T = 300K$.

- [8] L. Qiu and S. J. Hagen, *Chem. Phys.* **312**, 327 (2005).
- [9] D. Doucet, A. Roitberg, and S. J. Hagen, *BioPhys. J* **92**, 2281 (2007).
- [10] M. Volk, L. Milanesi, J. P. Waltho, C. A. Hunter, and G. S. Beddard, *Phys. Chem. Chem. Phys.* **17**, 762 (2015).
- [11] A. Soranno, B. Buchli, D. Nettels, R. R. Cheng, S. Müller-Späth, S. H. Pfeil, A. Hoffmann, E. A. Lipman, D. E. Makarov, and B. Schuler, *Proc. Natl. Acad. Sci.* **109**, 17800 (2012).
- [12] U. M. Yasin, P. Sashi, and A. K. Bhuyan, *J. Phys. Chem. B* **117**, 12059 (2013).
- [13] G. Wilemski and M. Fixman, *J. Chem. Phys.* **60**, 866 (1974).
- [14] A. Szabo, K. Schulten, and Z. Schulten, *J. Chem. Phys.* **72**, 4350 (1980).
- [15] T. Bandyopadhyay and S. K. Ghosh, *J. Chem. Phys.* **116**, 4366 (2002).
- [16] T. Bandyopadhyay and S. K. Ghosh, *J. Chem. Phys.* **119**, 572 (2003).
- [17] J. J. Portman, *J. Chem. Phys.* **118**, 2381 (2003).
- [18] I. M. Sokolov, *Phys. Rev. Lett.* **90**, 080601 (2003).
- [19] N. M. Toan, G. Morrison, C. Hyeon, and D. Thirumalai, *J. Phys. Chem. B* **112**, 6094 (2008).
- [20] G. Srinivas, B. Bagchi, and K. L. Sebastian, *J. Chem. Phys.* **116**, 7276 (2002).
- [21] D. Sarkar, S. Thakur, Y.-G. Tao, and R. Kapral, *Soft Matter*. **10**, 9577 (2014).
- [22] J. Shin, A. G. Cherstvy, and R. Metzler, *Soft Matter* **11**, 472 (2015).
- [23] A. G. Cherstvy, *J. Phys. Chem. B* **115**, 4286 (2011).
- [24] J. Shin, A. G. Cherstvy, and R. Metzler, *ACS Macro Lett.* **4**, 202 (2015).
- [25] T. Cellmer, E. R. Henry, J. Hofrichter, and W. E. Eaton, *Proc. Natl. Acad. Sci.* **105**, 18320 (2008).
- [26] A. Borgia, B. G. Wensley, A. Soranno, D. Nettels, M. B. Borgia, A. Hoffmann, S. H. Pfeil, E. A. Lipman, J. Clarke, and B. Schuler, *Nat. Commun.* **3**, 1195 (2012).
- [27] D. E. Makarov, *J. Chem. Phys.* **132**, 035104 (2010).
- [28] R. R. Cheng, A. T. Hawk, and D. E. Makarov, *J. Chem. Phys.* **138**, 074112 (2013).
- [29] N. Samanta and R. Chakrabarti, *Chem. Phys. Letts.* **582**, 71 (2013).
- [30] N. Samanta, J. Ghosh, and R. Chakrabarti, *AIP Adv.* **4**, 067102 (2014).
- [31] N. Samanta and R. Chakrabarti, *Physica A* **436**, 377 (2015).
- [32] T. R. Einert, C. E. Sing, A. Alexander-Katz, and R. R. Netz, *Euro. Phys. J. E* **34**, 1 (2011).
- [33] J. C. F. Schulz, L. Schmidt, R. B. Best, J. Dzubiella, and R. R. Netz, *J. Am. Chem. Soc.* **134**, 6273 (2012).

- [34] A. Erbas and R. R. Netz, *BioPhys. J* **103**, 1285 (2013).
- [35] D. de Sancho, A. Sirur, and R. B. Best, *Nat. Commun.* **5**, 4307 (2014).
- [36] I. Echeverria, D. E. Makarov, and G. A. Papoian, *J. Am. Chem. Soc.* **136**, 8708 (2014).
- [37] W. Zheng, D. D. Sancho, T. Hoppe, and R. B. Best, *J. Am. Chem. Soc.* **137**, 3283 (2015).
- [38] J. C. F. Schulz, M. S. Miettinen, and R. R. Netz, *J. Phys. Chem. B* **119**, 4565 (2015).
- [39] P. G. de Gennes, *Scaling Concepts in Polymer Physics* (Cornell University Press, Ithaca, N. Y., 1985).
- [40] P. J. Flory, *Principles of Polymer Chemistry* (Cornell University Press, 1953).
- [41] P. J. Flory, *Statistical mechanics of chain molecules* (Interscience Publishers, 1969).
- [42] M. Rubinstein and R. H. Colby, *Polymer Physics* (Oxford University Press, 2003).
- [43] J. Sung, J. Lee, and S. Lee, *J. Chem. Phys.* **118**, 414 (2003).
- [44] P. Debnath and B. J. Cherayil, *J. Chem. Phys.* **120**, 2482 (2004).
- [45] J.-H. Kim, W. Lee, J. Sung, and S. Lee, *J. Phys. Chem. B* **112**, 6250 (2008).
- [46] W. Yu and K. Luo, *J. Chem. Phys.* **142**, 124901 (2015).
- [47] M. Buscaglia, L. J. Lapidus, W. A. Eaton, and J. Hofrichter, *BioPhys. J* **91**, 276 (2006).
- [48] D. Panja and G. T. Barkema, *J. Chem. Phys.* **131**, 154903 (2009).
- [49] J. E. Kohn, I. S. Millett, J. Jacob, B. Zagrovic, T. M. Dillon, N. Cingel, R. S. Dothager, S. Seifert, P. Thiyagarajan, T. R. Sosnick, et al., *Proc. Natl. Acad. Sci. U.S.A.* **101**, 12491 (2004).
- [50] H. Hofmann, A. Soranno, A. Borgia, K. Gast, D. Nettels, , and B. Schuler, *Proc. Natl. Acad. Sci. U.S.A.* **109**, 16155 (2012).
- [51] M. Doi and S. F. Edwards, *The Theory of Polymer Dynamics* (Clarendon Press. Oxford, 1988).
- [52] T. Kawakatsu, *Statistical Physics of Polymers An Introduction* (Springer, 2004).
- [53] S. Gooßen, A. R. Braś, W. Pyckhout-Hintzen, A. Wischnewski, D. Richter, M. Rubinstein, J. Roovers, P. J. Lutz, Y. Jeong, T. Chang, et al., *Macromolecules* **48**, 1598 (2015).
- [54] B. S. Khatri and T. C. B. McLeish, *Macromolecules* **40**, 6770 (2007).
- [55] A. Amitai and D. Holcman, *Phys. Rev. Lett.* **110**, 248105 (2013).
- [56] R. Chakrabarti, *Chem. Phys. Lett.* **502**, 107 (2011).
- [57] M. Doi, *Chem. Phys.* **9**, 455 (1975).
- [58] R. Chakrabarti, *Physica A* **391**, 4081 (2012).

- [59] R. Chakrabarti, *Physica A* **391**, 5326 (2012).
- [60] P. Bhattacharyya, R. Sharma, and B. J. Cherayil, *J. Chem. Phys.* **136**, 234903 (2012).
- [61] K. P. Santo and K. L. Sebastian, *Phys. Rev. E.* **80**, 061801 (2009).
- [62] A. Möglich, K. Jorder, and T. Kiefhaber, *Proc. Natl. Acad. Sci.* **103**, 12394 (2006).
- [63] C. Domb, J. Gills, and G. Willmers, *Proc. Phys. Soc. Lond.* **85**, 625 (1965).
- [64] B. Bagchi, *Molecular Relaxation in Liquids* (Oxford University Press, 2012).
- [65] K. L. Sebastian, *Phys. Rev. A* **46**, R1732 (1992).
- [66] A. Debnath, R. Chakrabarti, and K. L. Sebastian, *J. Chem. Phys.* **124**, 204111 (2006).
- [67] R. W. Pastor, R. Zwanzig, and A. Szabo, *J. Chem. Phys.* **105**, 3878 (1996).
- [68] G. Srinivas, A. Yethiraj, and B. Bagchi, *J. Chem. Phys.* **114**, 9170 (2001).
- [69] B. Friedman and B. O'Shaughnessy, *Phys. Rev. A* **40**, 5950 (1989).
- [70] D. Nettels, A. Hoffmann, and B. Schuler, *J. Phys. Chem. B* **112**, 6137 (2008).
- [71] S. Müller-Späth, A. Soranno, V. Hirschfeld, H. Hofmann, S. Rügger, L. Reymond, D. Nettels, and B. Schuler, *Proc. Natl. Acad. Sci.* **107**, 14609 (2010).
- [72] J. L. Englanda and G. Haran, *Proc. Natl. Acad. Sci.* **107**, 14519 (2010).